Preprints (www.preprints.org) | NOT PEER-REVIEWED | Posted: 30 July 2018 doi:10.20944/preprints201807.0592.v1

Peer-reviewed version available at *Catalysts* **2018**, *8*, 340; doi:10.3390/catal8080340

Article

Low-temperature electrocatalytic conversion of CO_2 to liquid fuels: effect of the Cu particle size

Antonio de Lucas-Consuegra[1]*, Juan Carlos Serrano-Ruiz[2], Nuria Gutiérrez-Guerra[1], José Luis Valverde[1]

[1] Department of Chemical Engineering, School of Chemical Sciences and Technologies, University of Castilla-La Mancha, Avda. Camilo José Cela 12, 13005 Ciudad Real, Spain

[2] Department of Engineering, Universidad Loyola Andalucía, Energía Solar, 1. Edifs. E, F and G, 41014, Seville, Spain

* Correspondence: Antonio.lconsuegra@uclm.es; Tel.: +34-926295300

Abstract: A novel gas-phase electrocatalytic system based on a low-temperature proton exchange membrane (Sterion) was developed for the gas phase electrocatalytic conversion of CO_2 to liquid fuels. This system achieved gas-phase electrocatalytic reduction of CO_2 at low temperatures (below 90 ºC) over a Cu cathode by using water electrolysis-derived protons generated in-situ on an IrO_2 anode. Three Cu-based cathodes with varying metal particle sizes were prepared by supporting this metal on an activated carbon at three loadings (50, 20, and 10 wt%; 50%Cu-AC, 20%Cu-AC, and 10%Cu-AC, respectively). The cathodes were characterized by N_2 adsorption–desorption, temperature-programmed reduction (TPR), and X-ray diffraction (XRD) whereas their performance towards the electrocatalytic conversion of CO_2 was subsequently studied. The membrane electrode assembly (MEA) containing the cathode with the largest Cu particle size (50%Cu-AC, 40 nm) showed the highest CO_2 electrocatalytic activity per mole of Cu, with methyl formate being the main product. This higher electrocatalytic activity was attributed to the lower Cu–CO bonding strength over large Cu particles. Different product distributions were obtained over 20%Cu-AC and 10%Cu-AC, with acetaldehyde and methanol being the main reaction products, respectively. The CO_2 consumption rate increased with the applied current and the reaction temperature.

Keywords: CO_2 electroreduction; CO_2 valorization; Cu catalyst; Particle size; PEM; Acetaldehyde production; Methanol production

1. Introduction

Fossil fuels and biomass are the most common feedstocks for the production of liquid fuels. Since burning of these feedstocks results in CO_2 emissions into the atmosphere, it is necessary to develop strategies for the upgrading of this gas into useful products. One of these approaches involves the recycling of CO_2 into sustainable hydrocarbon fuels [1] by different methods such as catalytic processes (e.g., hydrogenation to alkanes, alkenes or other oxygenated, or reforming with hydrocarbons) [2], biological processes [3], microwave and plasma systems [4–6], and photocatalytic and electrocatalytic routes [7]. Among these methods, the electrochemical reduction of CO_2 is highly interesting since it allows to directly transform CO_2 to syngas and light hydrocarbons with electricity, which may be obtained from renewable energy sources [1, 8, 9]. This approach is advantageous in that electrochemical cell reactors are typically compact, modular, and easy to scale-up. While electrolysis of CO_2 and/or H_2O can be carried out in solid oxide cells (SOCs) [10], the high temperatures required for these systems to operate (above 600 ºC) usually result in catalyst sintering and stability losses. In addition, high-temperature CO_2-H_2O co-electrolysis produces syngas as the only product, and further conversion steps (e.g., Fischer–Tropsch synthesis) are required to produce hydrocarbon fuels. Alternatively, low-temperature electrolyzers containing protonic exchange membranes (PEM) have been proposed to directly transform CO_2 into hydrocarbons and oxygenates [11–13]. Despite the overall single-pass conversions are typically low in these reactors, the unreacted CO_2 can be easily separated from the liquid fuels and recycled again to the reactor. The mild working

Preprints (www.preprints.org) | NOT PEER-REVIEWED | Posted: 30 July 2018 doi:10.20944/preprints201807.0592.v1

Peer-reviewed version available at Catalysts 2018, 8, 340; doi:10.3390/catal8080340

conditions of these systems (typically below 90 ºC and atmospheric pressure) facilitate the utilization of renewable energies such as solar heating and electrical energy for driving the electrochemical process. Moreover, unlike conventional catalytic hydrogenation of CO_2, PEM-based electrolyzers do not require external hydrogen since CO_2 directly reacts with the protons produced in-situ by water electrolysis [7]. These advantages have motivated researchers to investigate on gas-phase low-temperature CO_2 electroreduction [9, 13–16], opening the way for incorporating renewable energies into the value chain of chemical industries. Prof. Centi has developed most of these works with Pt, Fe, and Cu catalyst supported on a variety of carbonaceous materials such as carbon black, carbon nanofibers, and graphene, among others.

In this work, we carried out the electroreduction of CO_2 in the gas phase at low temperature over Cu cathodes. We performed a systematic study with three different Cu-based cathodic catalysts supported on a high surface area activated carbon. The main objective of the work was to study the influence of the Cu particle size on the electrocatalytic activity of the system. With this aim, three different membrane electrode assemblies (MEAs) were fabricated with three Cu cathodic catalysts having varying metal loadings and particle sizes. These MEAs were characterized and tested for the electrocatalytic conversion of CO_2 into synthetic fuels.

2. Results and discussion

2.1. Characterization of the Cu powder catalysts and the Cu electrodes

The different Cu powders and Cu cathodic-catalysts were characterized by N_2 adsorption–desorption, atomic absorption spectroscopy (AAS), temperature-programmed reduction (TPR), and X-ray diffraction (XRD). Table 1 shows the physicochemical properties of the activated carbon support and the three Cu cathodic-catalysts.

Table 1. Physicochemical properties of the support material, the catalysts and the fresh electrodes.

Sample	Powder metal loading / wt%	Electrode metal weight / mgcm^{-2}	Surface area / m^{2}g^{-1}	Total pore volume /cm^3 g^{-1}	TPR-T_{max} / ºC	Mean particle size from XRD / nm
AC	-	-	866	0.293	-	-
50%Cu-AC	55	0.22	773	0.186	171	40
20%Cu-AC	19	0.18	797	0.260	185	14
10%Cu-AC	12	0.16	817	0.274	193	12

The main difference between the three Cu cathodic catalysts is the metal loading. Thus, AAS revealed metal loadings of 55, 19 and 12 wt% corresponding to electrode metal weights of 0.22, 0.18, and 0.16 mg cm^{-2} for the 50%Cu-AC, 20%Cu-AC, and 10%Cu-AC cathodic-catalysts, respectively. The electrocatalytic rates discussed below were normalized to the corresponding metal weight of the electrode.

The surface area and total pore volume of the different Cu cathodic-catalysts were determined by N_2 adsorption–desorption (Table 1). The activated carbon support showed high Langmuir areas and total pore volumes (866 m^{2}g^{-1} and 0.293 cm^{2}g^{-1}, respectively), as previously reported in the literature [17, 18]. As shown in Table 1, metal addition resulted in an important decrease of both the surface area and the total pore volume. As expected, the surface area and the total pore volume

Peer-reviewed version available at Catalysts 2018, 8, 340; doi:10.3390/catal8080340

decreased with the metal loading, probably as a result of partial pore blockage by the metal particles [18, 19]. Combined IUPAC types I and IV N_2 adsorption–desorption isotherms (not shown) were obtained in all cases, revealing the presence of a microporous structure.

The TPR profiles of 50%Cu-AC, 20%Cu-AC and 10%Cu-AC and the activated carbon support are shown in Figure 1. These TPR profiles can be explained can result from a sequential Cu reduction as follows: $Cu^{2+} \rightarrow Cu^{+} \rightarrow Cu^{0}$ [20]. The first two reduction peaks at 171–193 ºC and 223–276 ºC (depending on the catalyst) can be attributed to the reduction of the more dispersed Cu particles and the reduction of CuO(II), respectively. The third reduction peak appeared at 316–380 ºC can be assigned to the reduction of Cu_2O(I). Finally, the peaks at higher temperatures are typically associated with the gasification of activated carbon and the reduction of surface oxygenated groups on the activated carbon support [21, 22]. The temperature of the most intense consumption peak (T_{max}) is given in Table 1. The TPR profiles revealed that the interaction between the metal phase and the support varied depending on the metal particle size. Thus, stronger interactions were obtained for those catalysts having smaller Cu particles since T_{max} decreased with the Cu particle size (Table 1) [20, 23, 24]. Thus, the reducibility of the catalysts followed the sequence: 50%Cu-AC < 20%Cu-AC < 10%Cu-AC. Furthermore, in view of the TPR profiles, 400 ºC was selected as a suitable reduction temperature for ensuring complete metal activation while maintaining the surface properties of the support.

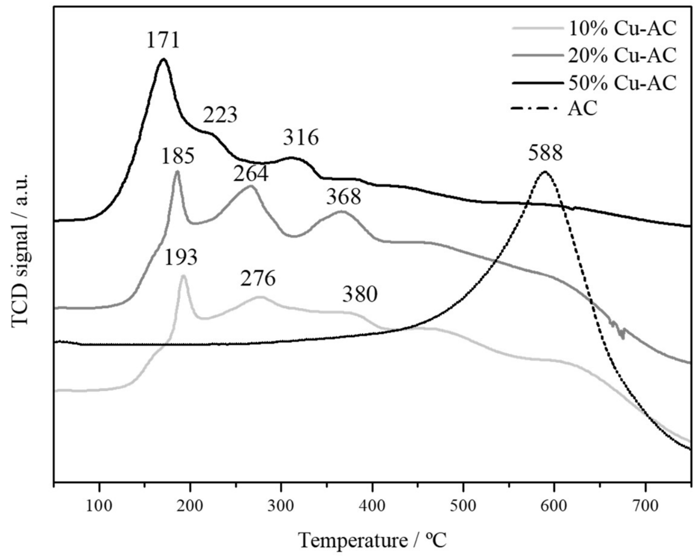

Figure 1. TPR profiles of the fresh catalysts and the activated carbon support.

Figure 2 shows the XRD patterns of the powder catalyst 50 % Cu-AC before and after the reduction treatment at 400 ºC. No significant differences were appreciated between the three Cu-AC powder catalysts. As shown in Figure 2.a, diffraction peaks corresponding to metallic copper (Cu) and copper oxide (Cu_2O and CuO) were observed before the reduction treatment. The main diffraction Cu peaks were (111), (200), (220), and (331) observed at 43.3, 50.4, 74.1, and 89.8º, respectively. These peaks are associated with a metallic Cu phase with face-centered cubic (FCC) crystalline structure (JCPDS, 85-1326). Diffraction peaks corresponding to Cu_2O (JCPDS, 78-2076) and CuO (JCPDS, 80-1917) were also observed, in line with the TPR results (Figure 1). However, these peaks were lower in intensity as compared to those of metallic copper. Figure 2.b shows the XRD patterns of the catalysts after the reduction treatment. As shown by the XRD patterns, only peaks corresponding to metallic Cu were observed at 2θ = 43.3, 50.4, 74.1, and 90º for the (111), (200), (220), and (331) planes. These results revealed that Cu was completely reduced at 400 ºC, as anticipated by the TPR profiles. Additionally, the metal precursor was completely calcined, since no peaks corresponding to the metal precursor were observed in the XRD patterns. The mean Cu particle sizes

Peer-reviewed version available at Catalysts 2018, 8, 340; doi:10.3390/catal8080340

of the different catalysts were estimated using the Scherrer equation, and the results are summarized in Table 1. As expected, the mean Cu particle size increased significantly with the metal loading. The Cu particle sizes obtained herein (10–40 nm) were similar to those determined for similar electrocatalytic systems prepared by direct impregnation with Cu precursor solutions [16, 17, 25].

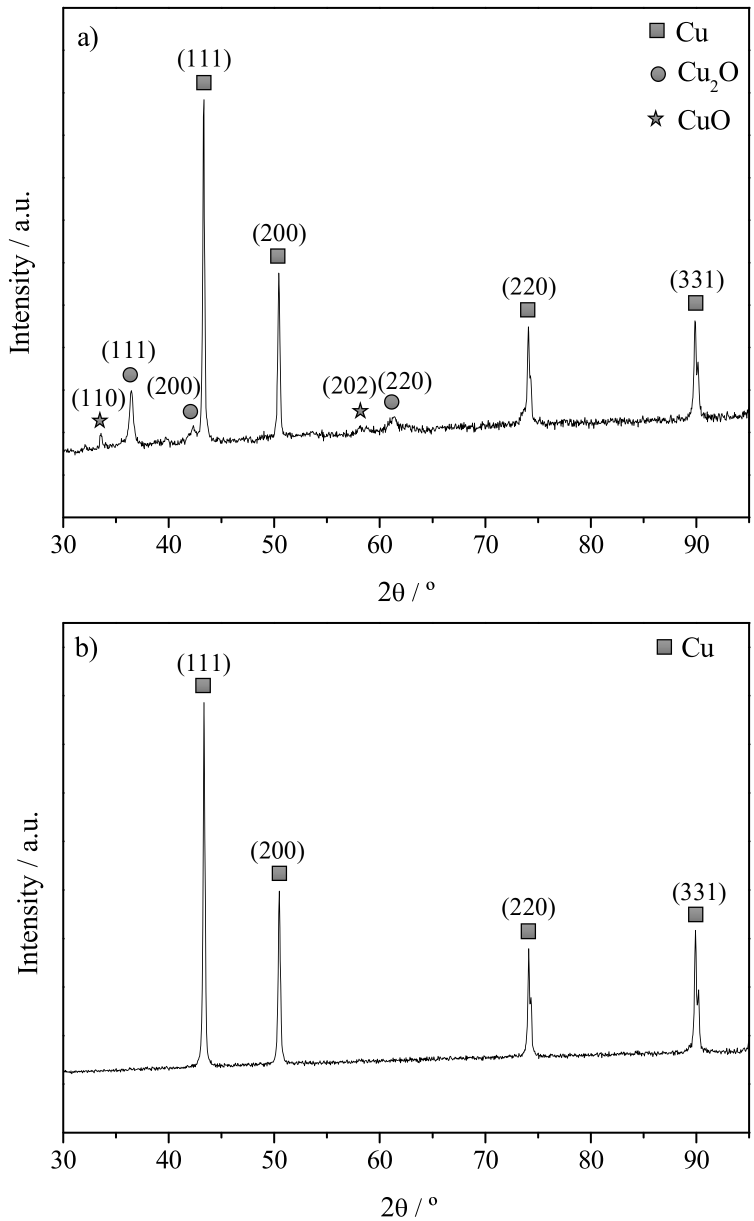

Figure 2. XRD patterns of 50%Cu-AC supported on carbon paper substrates: (a) before reduction at 400 ºC and (b) after reduction at 400 ºC.

2.2. CO_2 conversion electrocatalytic experiments

Figure 3 shows the production rates of different compounds as a function of the time on stream during the electroreduction of CO_2 at a constant applied current of -20 mA and 90 ºC. Note that no products were obtained under open circuit conditions (OCC, no current application). A constant

Peer-reviewed version available at Catalysts 2018, 8, 340; doi:10.3390/catal8080340

current of -20 mA was subsequently applied at 90 ºC for approximately 350 min under the same reaction atmosphere. This polarization was maintained until products were obtained at a steady state rate. During this current application step, hydrogen (not shown in Figure 3, reaction (2)) and different products such as methanol, acetaldehyde, methyl formate, acetone, and n-propanol were obtained by reactions (3)–(7), respectively:

$$2H^{+} + 2e^{-} \rightarrow H_2 \quad (2)$$

$$CO_2 + 6H^{+} + 6e^{-} \rightarrow CH_3OH + H_2O \quad (3)$$

$$2CO_2 + 10H^{+} + 10e^{-} \rightarrow C_2H_4O + 3H_2O \quad (4)$$

$$2CO_2 + 8H^{+} + 8e^{-} \rightarrow C_2H_4O_2 + 2H_2O \quad (5)$$

$$3CO_2 + 16H^{+} + 16e^{-} \rightarrow C_3H_6O + 5H_2O \quad (6)$$

$$3CO_2 + 18H^{+} + 18e^{-} \rightarrow C_3H_8O + 5H_2O \quad (7)$$

Most of these products have been previously obtained during the electrocatalytic conversion of CO_2 on Fe, Co, Pt, and Cu supported on carbon nanotubes [15, 16, 26–28] and Cu supported on different carbonaceous supports (activated carbon, carbon nanofibers, and graphite) [17] at similar temperatures. These products reached maximum production rates after ca. 300 min on stream and decreased upon OCC. A slow dynamic behaviour was observed (the steady state was reached after 4–5 h of reaction), and this can be attributed to the high residence times used herein.

The configuration used herein is advantageous in that it allows direct supply of H^+ (more reactive than H_2) to the cathodic side of the cell. This configuration allows lower temperatures (around 90 ºC) as compared to catalytic CO_2 hydrogenation processes (above 250 ºC) [21, 29–31].

Finally, in all experiments, the cathodic side of the cell was purged with N_2 (30 NmL min^{-1}) and returned to OCC in order to remove all the products for subsequent reaction experiments. Sample 50%Cu-AC showed the highest intrinsic electrocatalytic activity among the three cathodic-catalyst studied herein. This higher electrocatalytic activity can be associated to the higher Cu particle size of 50%Cu-AC. Thus, large Cu particles have been previously reported to favor the formation of reaction products by reducing the strength of the metal–CO interaction [32]. In the electroreduction of CO_2, CO_2 is adsorbed on active centers and subsequently converted into CO and O_2. Since this CO adsorbed is more reactive than CO_2, it reacts with protons to generate the different products observed. This reaction is favored on large Cu particles. Since small Cu particles adsorb CO more strongly than large particles, the subsequent reaction of CO is hindered on small Cu particles, leading to CO and H_2 as the only products [32].

With regard to the composition of the reaction products, methyl formate was the main reaction product over 50%Cu-AC, followed by acetaldehyde and methanol. Acetaldehyde and methanol were the main reaction products obtained over samples 20%Cu-AC and 10%Cu-AC, respectively. In line with our results, acetaldehyde and methanol were previously obtained as main products over Cu-AC catalysts [17]. In the case of catalyst 50%Cu-AC, the high Cu particle size favored the production of methyl formate by dehydrogenation of methanol (Reaction (8), as previously reported [33].

$$2CH_3OH \rightarrow HCOOCH_3 + 2H_2 \quad (8)$$

Peer-reviewed version available at Catalysts 2018, 8, 340; doi:10.3390/catal8080340

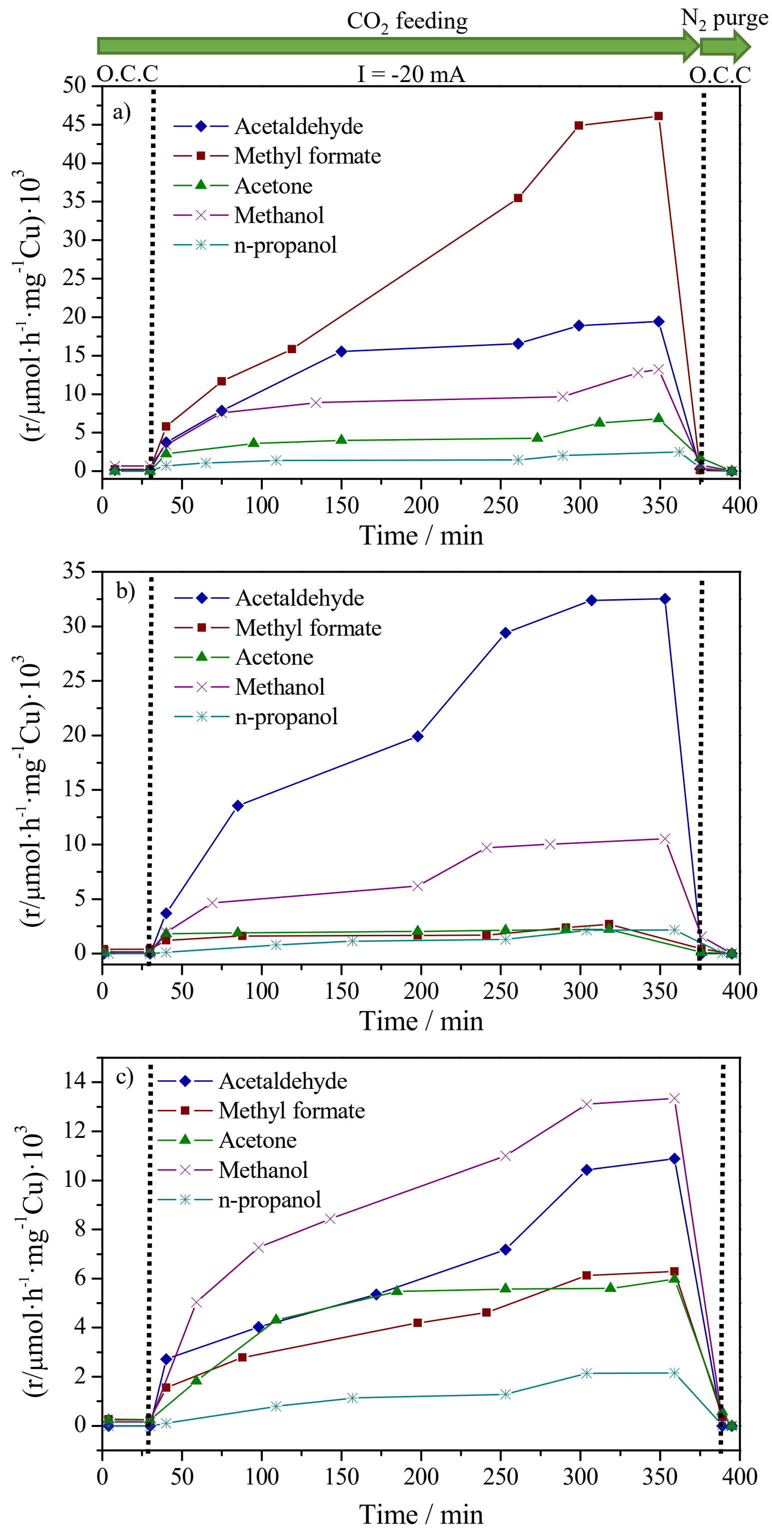

Figure 3. Time-on-stream variation of the rate of production for the different products at a constant current of -20 mA over the cathodic-catalysts on carbon paper substrates: (a) 50%Cu-AC, (b) 20%Cu-AC, and (c) 10%Cu-AC. Conditions: temperature = 90 ºC, $F_{(CO_2)}$, cathode = 1.65 NmL·min^{-1} y $F_{(H_2O)}$, anode = 6 NmL·min^{-1}.

Figures 4a and b summarize the effect of the applied current and the reaction temperature on the steady state CO_2 consumption rate (after 350 min of polarization), respectively. The reaction rates

Preprints (www.preprints.org) | NOT PEER-REVIEWED | Posted: 30 July 2018 doi:10.20944/preprints201807.0592.v1

Peer-reviewed version available at *Catalysts* **2018**, *8*, 340; doi:10.3390/catal8080340

were normalized by the amount of Cu deposited on each cathodic-catalyst. In line with the previous experiments, sample 50%Cu-AC showed larger electrocatalytic activities than samples 20%Cu-AC and 10%Cu-AC for all the reaction conditions studied. As expected, the consumption rate of CO_2 increased with the applied current, most likely because of an increase in the electrochemical supply of H^+. In line with previous studies [15], an increase in the reaction temperature also resulted in higher electrocatalytic activities for all the catalysts tested. While the kinetics of the electrochemical reactions can be improved by increasing the temperature [34], the protonic membrane prevented us from testing the system above 90 ºC since its stability and conductivity under appropriate humidity conditions is not ensured at these conditions.

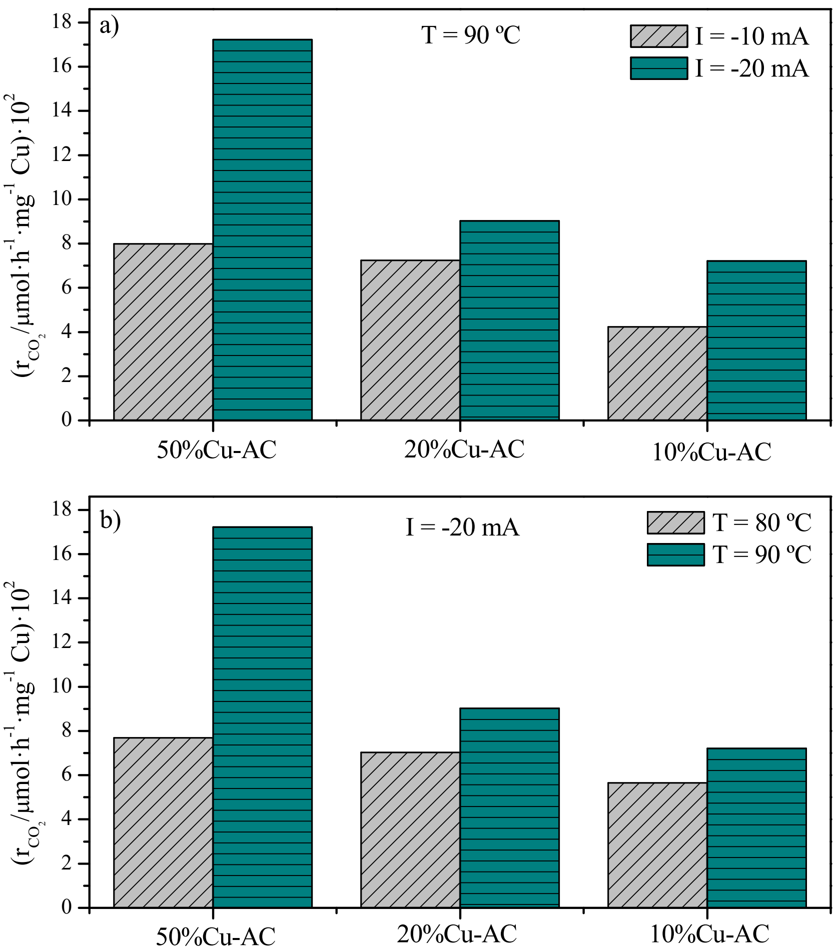

Figure 4. (a) Effect of the current at 90 ºC and (b) temperature at I= -20 mA on the steady state CO_2 consumption rate for the cathodic-catalysts 50%Cu-AC, 20%Cu-AC, and 10%Cu-AC. Conditions: $F_{(CO_2)}$, cathode = 1.65 NmL·min^{-1} y $F_{(H_2O)}$, anode = 6 NmL·min^{-1}.

Finally, we calculated the energy consumption for the three different cathodic-catalysts evaluated. The three different MEAs were compared at 90 ºC and -20 mA. The overall energy consumption for CO_2 conversion (kW·h·mol^{-1} CO_2) and the energy consumption for the production of methanol (kW·h·mol^{-1} CH_3OH), acetaldehyde (kW·h·mol^{-1} CH_3CHO), and methyl formate (kW·h·mol^{-1} HCO_2CH_3) were calculated. As indicated above, the cathodic-catalyst with the highest metal loading, 50%Cu-AC, showed the highest electrocatalytic activity. This catalyst showed the lowest energy consumption for the conversion of CO_2 (119.01 kW·h·mol-1) among the catalysts tested. In addition, the MEA containing 50%Cu-AC consumed less energy per kg of methanol, acetaldehyde, and methyl formate (1549, 1054, and 444 kW·h·mol^{-1}, respectively) than the other two ones.

Preprints (www.preprints.org) | NOT PEER-REVIEWED | Posted: 30 July 2018 doi:10.20944/preprints201807.0592.v1

Peer-reviewed version available at Catalysts 2018, 8, 340; doi:10.3390/catal8080340

3. Materials and Methods

Cu catalysts supported on activated carbon were used as cathodes for the electrochemical reduction of CO_2, while Ir (IV) oxide (IrO_2) supported on carbon was used as a cell anode.

A commercial high surface area activated carbon (Sigma Aldrich) was used as a support. Metal particles were deposited on the activated carbon by the impregnation method. The support was placed in a glass vessel and kept under vacuum at room temperature for 2 h to remove water and other compounds adsorbed. A known volume of an ethanolic solution of $Cu(NO_3)_3{\cdot}3H_2O$ (Panreac) was then poured over the sample. The solvent was subsequently removed by vacuum evaporation at 90 ºC for 2 h in a rotary evaporator. The catalysts were dried at 120 ºC overnight, calcined for 2 h at 350 ºC in a N_2 atmosphere, and finally reduced in H_2 at 400 ºC for 2 h with a heating rate of 5 $ºC{\cdot}min^{-1}$. Three different catalysts were prepared with total Cu loadings of 50, 20, and 10 wt% (50%Cu-AC, 20%Cu-AC, and 10%Cu-AC, respectively).

The catalyst inks were prepared by mixing appropriate amounts of the different catalysts (IrO_2 commercial catalyst powders (Alfa Aesar, 99%) for the anode, and Cu-activated-carbon powder for the cathode) with a Nafion solution (5 wt%, Aldrich chemistry, Nafion® 117 solution) in isopropanol (Sigma Aldrich) containing a blinder/solvent volume ratio of 0.04. IrO_2 was selected as an anode because of its superior water electro-oxidation ability in conventional PEM electrolyzers [17]. Then, the different inks were deposited on carbon paper (Fuel Cell Earth) substrates with a geometric surface area for both electrodes of 12.56 cm^2 (circular electrode of 4 cm in diameter) at 65 ºC. The metal loading was 0.5 $mg{\cdot}cm^{-2}$ for each electrode after drying. A proton conducting Sterion® membrane of 185 μm in thickness (Hydrogen Works) was used as the electrolyte (i.e., H+ conductor material). Prior to use, the Sterion® membrane was successively immersed at 100 ºC for 2 h in H_2O_2 (to remove organic impurities) and H_2SO_4 (to promote activation), and in deionized water to remove traces of the previous solutions. Then, the MEA was prepared by sandwiching the membrane between the electrodes. Finally, the whole system was hot-pressed (GRASEBY SPEAC) at 120 ºC and a pressure of 1 metric ton for 3 min.

The Cu metal loading on the cathodic powder catalysts was determined by AAS using a SPECTRA 220FS analyzer. The sample (ca. 0.5 g) was dissolved in a mixture containing 2 mL of HCl, 3 mL of HF, and 2 mL of H_2O_2 followed by microwave digestion at 250 ºC. The surface area and volume porosity measurements of the support and powder catalysts were conducted on a Micromeritics ASAP 2010. N_2 was used as the sorbate at -193 ºC and the microporosity of the materials was evaluated by the Howath–Kawazoe (HK) method. Prior to the analyses, the samples were outgassed at 180 ºC under vacuum ($5{\cdot}10^{-3}$ Torr) for 12 h. TPR experiments were conducted on a commercial Micromeritics AutoChem 2950 HP unit provided with a thermal conductivity (TCD) detector. The samples (ca. 0.15 g) were loaded into a U-shaped tube and ramped from room temperature up to 900 ºC (10 ºC min^{-1}) under a reducing H_2/Ar gas mixture of 17.5% v/v (60 cm^3 min^{-1}). XRD analyses were conducted on the Cu-AC powder catalysts before and after reduction with a Philips PW-1710 instrument, using Ni-filtered Cu Kα radiation (λ = 1.5404 Å). The samples were scanned at a rate of $0.02º{\cdot}step^{-1}$ over a 2θ range of 20–80º (scan time 2 $s{\cdot}step^{-1}$) and the diffractograms were compared with the corresponding JCPDS-ICDD references.

2.2. Electrocatalytic activity measurements

Electrocatalytic CO_2 conversion experiments were carried out in a lab-scale continuous electrochemical cell reactor operating at atmospheric pressure [17]. Water was introduced into the anode side of the cell by flowing N_2 through a saturator to achieve liquid/vapor equilibrium. The water content in the anodic chamber of reaction mixture (25 % H_2O/N_2) was controlled by the vapor pressure of water at the temperature of the saturator (65 ºC). All lines downstream the saturator were heated above 100 ºC to prevent condensation. In the anode side, water electrolysis was carried out on

Peer-reviewed version available at *Catalysts* **2018**, *8*, 340; doi:10.3390/catal8080340

IrO_2 to generate protons across the Sterion® membrane. The water stream was also used to hydrate the Sterion® membrane and keep its proton conductivity properties [16]. The cathodic part of the cell operates under a gas flow of pure CO_2 (Praxair, Inc. certified standards 99.999% purity). Both gas flow rates (N_2 for the anode and CO_2 for the cathode) were controlled by a set of mass flowmeters (Brooks 5850 E and 5850 S, respectively). The electrocatalytic experiments were carried out at atmospheric pressure with an overall gas flow rate of 0.5 NmL min^{-1} of CO_2 for the cathodic stream and 6 NmL min^{-1} for the anodic stream (60 % H_2O/N_2) at different temperatures (80 and 90 ºC, optimum operation values for the Sterion membrane). The reactant and products released from the cathodic chamber of the cell were analyzed by using a double channel gas chromatograph (Bruker 450-GC) equipped with Hayesep Q-Molsieve 13X consecutive columns and flame ionization detectors (FIDs). Hydrogen, methanol, acetaldehyde, methyl formate, acetone, and n-propanol were the reaction products detected. The carbon atom balance closed within a 5 % error. A potentiostat/galvanostat (Voltalab 21, Radiometer Analytical) was used to supply a constant current (from -10 to -30 mA) between the electrodes, which were connected using gold wires.

4. Conclusions

Three different Cu-based cathodic-catalysts with Cu loadings of 50, 20, and 10 wt% were synthesized by impregnation, characterized, and tested in the electrocatalytic conversion of CO_2.

50%Cu-AC showed the highest CO_2 electrocatalytic activity among the catalysts tested under all the explored reaction conditions. These results could be explained for the higher Cu particle size of this material. Considering that CO is an important intermediate in the process, large Cu particles are believed to favor electroreduction by weakening the metal–CO interaction.

Methyl formate was the main reaction product for 50%Cu-AC, while acetaldehyde and methanol were the main products for 20%Cu-AC and 10%Cu-AC, respectively. This fact can be attributed to the higher particle size of Cu that favored the production of methyl formate via dehydrogenation of methanol.

The CO_2 consumption rate increased with the applied current and the reaction temperature due to an enhancement of the kinetic of the electrocatalytic reactions.

Finally, 50%Cu-AC showed the highest electrocatalytic activity and the lowest energy consumption values for the conversion of CO_2 (119 kW·h·mol^{-1}). In addition, the MEA containing 50% of Cu consumed less energy per kg of methanol, acetaldehyde, and methyl formate than the other two MEAs containing less amount of Cu.

Acknowledgments: Financial Support from the Spanish "Ministerio de Ciencia e Innovación" (Project CTQ2016-75491-R) and from Abengoa Research is gratefully acknowledged. JCSR would like to acknowledge the Spanish Ministry of Science, Innovation and Universities for financial support under the Ramón y Cajal Program, grant RYC-2015-19230.

Author Contributions: J.L.V conceived the Project, N.G.G performed the experiments and J.C.S and A.D.L wrote the manuscript

Conflicts of Interest: The authors declare no conflict of interest. The founding sponsors had no role in the design of the study; in the collection, analyses, or interpretation of data; in the writing of the manuscript, and in the decision to publish the results.

References

1. Umeyama, T. & Imahori, H. Carbon nanotube-modified electrodes for solar energy conversion. *Energy Environ. Sci.* **2008**, *1(1)*, 120–133.
2. Bansode, A.; Urakawa, A. Towards full one-pass conversion of carbon dioxide to methanol and methanol-derived products. *J. Catal.* **2014**, *309*, 66–70.
3. Sekar, N.; Ramasamy, R. P. (2015). Recent advances in photosynthetic energy conversion. *J. Photochem. Photobiol. C-Photochem. Rev.* **2015**, *22*, 19–33.
4. Khiabani; N. H.; Yaghmaee, M. S.; Sarani, A.; Shokri, B. Synthesis-gas production from CH_4-CO_2-Ar via microwave plasma torch. *Adv. Stud. Theor. Phys.* **2012**, *6(26)*, 1273–1287.

Peer-reviewed version available at *Catalysts* **2018**, *8*, 340; doi:10.3390/catal8080340

5. Yu, Q.; Kong, M.; Liu, T.; Fei, J.; Zheng, X. Characteristics of the decomposition of CO_2 in a dielectric packed-bed plasma reactor. *Plasma Chem. Plasma Process.* **2012**, *32(1)*, 153–163.
6. Rahemi, N.; Haghighi, M.; Babaluo, A. A.; Jafari, M. F.; Allahyari, S. (2014). CO_2 reforming of methane over Ni-Cu/Al 2 O 3-ZrO 2 nanocatalyst: The influence of plasma treatment and process conditions on catalytic properties and performance. *Korean J. Chem. Eng.* **2014**, *31(9)*, 1553–1563.
7. Centi, G.; Perathoner, S. Opportunities and prospects in the chemical recycling of carbon dioxide to fuels. *Catal. Today* **2009**, *148(3-4)*, 191–205.
8. Albo, J.; Alvarez-Guerra, M.; Castaño, P.; Irabien, A.. Towards the electrochemical conversion of carbon dioxide into methanol. *Green Chem.* **2015**, *17(4)*, 2304–2324.
9. Centi, G.; Quadrelli, E. A.; Perathoner, S. Catalysis for CO_2 conversion: a key technology for rapid introduction of renewable energy in the value chain of chemical industries. *Energy Environ. Sci.* **2013**, *6(6)*, 1711–1731.
10. Graves, C.; Ebbesen, S. D.; Mogensen, M. (2011). Co-electrolysis of CO_2 and H_2O in solid oxide cells: performance and durability. *Solid State Ion* **2011**, *192(1)*, 398–403.
11. Blomen, E.; Hendriks, C.; Neele, F. Capture technologies: improvements and promising developments. *Energy Procedia* **2009**, *1(1)*, 1505–1512.
12. Yamanaka, I.; Tabata, K.; Mino, W.; Furusawa, T. Electroreduction of Carbon Dioxide to Carbon Monoxide by Co-pthalocyanine Electrocatalyst under Ambient Conditions. *ISIJ Int.* **2015**, *55(2)*, 399–403.
13. Ampelli, C.; Genovese, C.; Perathoner, S.; Centi, G. ; Errahali, M. ; Gatti, G.; Marchese, L. An electrochemical reactor for the CO_2 reduction in gas phase by using conductive polymer based electrocatalysts. *Chemical Engineering Transactions* **2014**, *41*, 13–18.
14. Lee, K.; Zhang, J., Wang; H.; Wilkinson, D. P. Progress in the synthesis of carbon nanotube-and nanofiber-supported Pt electrocatalysts for PEM fuel cell catalysis. *J. Appl. Electrochem.* **2006**, *36(5)*, 507–522.
15. Genovese, C.; Ampelli, C.; Perathoner, S.; Centi, G. Electrocatalytic conversion of CO_2 to liquid fuels using nanocarbon-based electrodes. *J. Energy Chem.* **2013**, *22(2)*, 202–213.
16. Genovese, C.; Ampelli, C.; Perathoner, S.; Centi, G. Electrocatalytic conversion of CO_2 on carbon nanotube-based electrodes for producing solar fuels. *J. Catal.* **2013**, *308*, 237–249.
17. Gutiérrez-Guerra, N.; Moreno-López, L.; Serrano-Ruiz, J. C.; Valverde, J. L.; de Lucas-Consuegra, A. Gas phase electrocatalytic conversion of CO_2 to syn-fuels on Cu based catalysts-electrodes. *Appl. Catal. B-Environ.* **2016**, *188*, 272–282.
18. Rodriguez-Reinoso, F. The role of carbon materials in heterogeneous catalysis. *Carbon* **1998**, *36(3)*, 159–175.
19. Molina-Sabio, M.; Perez, V.; Rodriguez-Reinoso, F. Impregnation of activated carbon with chromium and copper salts: Effect of porosity and metal content. *Carbon* **1994**, *32(7)*, 1259–1265.
20. Zhang, G.; Li, Z.; Zheng, H.; Fu, T.; Ju, Y.; Wang, Y. Influence of the surface oxygenated groups of activated carbon on preparation of a nano Cu/AC catalyst and heterogeneous catalysis in the oxidative carbonylation of methanol. *Appl. Catal. B-Environ.* **2015**, *179*, 95–105.
21. Díez-Ramírez, J.; Sánchez, P.; Rodríguez-Gómez, A.; Valverde, J. L.; Dorado, F. Carbon nanofiber-based palladium/zinc catalysts for the hydrogenation of carbon dioxide to methanol at atmospheric pressure. *Ind. Eng. Chem. Res.* **2016**, *55(12)*, 3556–3567.
22. Román-Martínez, M. C.; Cazorla-Amorós, D.; Linares-Solano, A.; De Lecea, C. S. M. TPD and TPR characterization of carbonaceous supports and Pt/C catalysts. *Carbon* **1993**, *31(6)*, 895–902.
23. Gil, S., Muñoz, L.; Sánchez-Silva, L.; Romero, A.; Valverde, J. L. Synthesis and characterization of Au supported on carbonaceous material-based catalysts for the selective oxidation of glycerol. *Chem. Eng. J.* **2011**, *172(1)*, 418–429.
24. Trépanier, M.; Dalai, A. K.; Abatzoglou, N. Synthesis of CNT-supported cobalt nanoparticle catalysts using a microemulsion technique: role of nanoparticle size on reducibility, activity and selectivity in Fischer–Tropsch reactions. *Appl. Catal. A-Gen.* **2010**, *374(1-2)*, 79–86.
25. Karelovic, A.; Ruiz, P. The role of copper particle size in low pressure methanol synthesis via CO_2 hydrogenation over Cu/ZnO catalysts. *Catal. Sci. Technol.* **2015**, *5(2)*, 869–881.
26. Genovese, C.; Ampelli, C.; Perathoner, S.; Centi, G. A gas-phase electrochemical reactor for carbon dioxide reduction back to liquid fuels. *Chemical Engineering Transactions* **2013**, *32(11)*, 289–294.
27. Gangeri, M.; Perathoner, S.; Caudo, S.; Centi, G.; Amadou, J.; Begin, D.; Schlögl, R. Fe and Pt carbon nanotubes for the electrocatalytic conversion of carbon dioxide to oxygenates. *Catal. Today* **2009**, *143(1-2)*, 57–63.

Peer-reviewed version available at *Catalysts* **2018**, *8*, 340; doi:10.3390/catal8080340

28. Centi, G.; Perathoner, S.; Winè, G.; Gangeri, M. Electrocatalytic conversion of CO_2 to long carbon-chain hydrocarbons. *Green Chem.* **2007**, *9(6)*, 671–678.
29. Ahouari, H.; Soualah, A.; Le Valant, A.; Pinard, L.; Magnoux, P.; Pouilloux, Y. Methanol synthesis from CO_2 hydrogenation over copper based catalysts. *React. Kinet. Mech. Catal.* **2013**, *110(1)*, 131–145.
30. Díez-Ramírez, J.; Valverde, J. L.; Sánchez, P.; Dorado, F. CO_2 hydrogenation to methanol at atmospheric pressure: influence of the preparation method of Pd/ZnO catalysts. *Catal. Lett*. **2016**, *146(2)*, 373–382.
31. Díez-Ramírez, J.; Dorado, F.; de la Osa, A. R.; Valverde, J. L.; Sánchez, P. Hydrogenation of CO_2 to methanol at atmospheric pressure over Cu/ZnO catalysts: influence of the calcination, reduction, and metal loading. *Ind. Eng. Chem. Res*. **2017**, *56(8)*, 1979–1987.
32. Reske, R.; Mistry, H.; Behafarid, F.; Roldan Cuenya, B.; Strasser, P. Particle size effects in the catalytic electroreduction of CO_2 on Cu nanoparticles. *J. Am. Chem. Soc.* **2014**, *136(19)*, 6978–6986.
33. Tonner, S. P.; Trimm, D. L.; Wainwright, M. S.; Cant, N. W. Dehydrogenation of methanol to methyl formate over copper catalysts. *Ind. Eng. Chem. Prod. Res. Dev.* **1984**, *23(3*), 384–388.
34. Caravaca, A.; Sapountzi, F. M.; de Lucas-Consuegra, A.; Molina-Mora, C.; Dorado, F.; Valverde, J. L. Electrochemical reforming of ethanol–water solutions for pure H_2 production in a PEM electrolysis cell. *Int. J. Hydrog. Energy* **2012**, *37(12)*, 9504–9513.